Chapter 6
Nonlinear Vibrations of a Beam with a Breathing Edge Crack

Ali C. Batihan and Ender Cigeroglu

Abstract In this paper, nonlinear transverse vibration analysis of a beam with a single edge crack is studied. In literature, edge cracks are generally modeled as open cracks, in which the beam is separated into two pieces at the crack location and these pieces are connected to each other with a rotational spring to represent the effect of crack. The open edge crack model is a widely used assumption; however, it does not consider the nonlinear behavior due to opening and closing of the crack region. In this paper, a beam like structure with a breathing type crack is studied. Due to the breathing nature of the crack, crack surfaces contact with each other for some period of the motion and separate in the rest of the cycle. This nonlinear behavior of the crack region is modeled by representing the system as a single degree of freedom system (SDOF) with a bilinear stiffness by Galerkin's Method. Nonlinear differential equations of motion obtained by using Euler-Bernoulli beam theory are converted into nonlinear algebraic equations by using harmonic balance method (HBM). Under the action of a harmonic forcing, the effect of crack parameters on the vibrational behavior of the cracked beam is presented.

Keywords Breathing crack • Euler-Bernoulli beam • Galerkin's method • Harmonic balance method

6.1 Introduction

Cracks in structures may propagate and cause catastrophic failures which do not give any visible sign before failure. Therefore, identification of cracks and determination of their location and properties is very important for life prediction of mechanical systems. Because of this importance, beams with edge cracks have been an increasingly growing area of research in the last 30 years. Review paper of Dimarogonas [1] provides a collection of researches that are carried out thus far, in which analysis methods for open and breathing crack, continuous crack beam theories, dynamic characteristics of cracked beams and studies of vibration of cracked plates are considered. In majority of the literature, cracked beam is separated into two segments at the crack location and then these two segments are connected to each other by rotational springs. The most common model used in the literature is beam with an open edge crack, where the Euler-Bernoulli beam theory is utilized. Khiem et al. [2] calculated the natural frequencies of a beam with arbitrary number of cracks by using a transfer matrix method. Another research considering arbitrary number of cracks as well as taking the effects of axial loads into account was carried out by Aydın [3]. Mermertaş [4] considered a mass attachment to see the change in the natural frequencies more effectively. Method of mass attachment was also considered by Zhong et al. [5] by the application of Rayleigh's and finite element methods. Also, Mazanoğlu et al. [6] studied a non-uniform cracked beam by applying Rayleigh-Ritz and finite element methods. Besides these approaches, alternative methods were also developed. Chondros et al. [7] developed a continuous theory of cracked beams where the flexibility due to crack region was distributed along the whole beam. Chati [8] carried out the modal analysis of a beam with breathing edge crack by using finite element method. The nonlinearity due to breathing effect was modeled by a piecewise linear stiffness. Chondros et al. [9] also studied a beam with breathing edge crack. In this study, vibration characteristics due to open period and closed period were combined as a bi-linear model. Authors indicated that fatigue cracks behave as breathing cracks if the preload is sufficient. In the study of Cheng et al. [10], the breathing crack was modeled with a time dependent stiffness. Baeza et al. [11] studied breathing crack by using an analytical approach, where utilizing beam modes a modal scale factor matrix is introduced which indicates the existence of cracks. In a more recent study, sub and super harmonics of a beam with a breathing crack is studied by Giannini et al. [12] and the approach is used for crack identification where the cracked beam is modeled by finite element method. The results obtained are also compared with the results of an experiment conducted.

A.C. Batihan • E. Cigeroglu (✉)
Department of Mechanical Engineering, Middle East Technical University, Ankara 06800, Turkey
e-mail: ender@metu.edu.tr

G. Kerschen (ed.), *Nonlinear Dynamics, Volume 1*, Conference Proceedings of the Society
for Experimental Mechanics Series, DOI 10.1007/978-3-319-15221-9_6

In this paper, transverse vibrations of a beam with a breathing edge crack is studied. The beam is modeled by Euler-Bernoulli beam theory and a SDOF representation of the cracked beam is obtained via Galerkin's method. For the application of Galerkin's method, trial functions that satisfy both natural and geometric boundary conditions are needed. Two different trial functions are used for this purpose. In case the crack is open, the first eigenfunction of a beam with an open crack is used whereas; the first eigenfunction of the undamaged beam is utilized in case the crack is closed. Using these two trial functions, a SDOF representation of the crack beam is obtained which contains a piecewise linear stiffness. Harmonic balance method (HBM) with multi harmonics is utilized for the solution of resulting nonlinear system and the effects of breathing crack and the parameters associated with it on higher harmonics are investigated.

6.2 Mathematical Modeling

Equation of motion of a continuous beam with an external forcing of $F(t)$ applied at location L_f can be written as follows using Euler-Bernoulli beam theory

$$EI\frac{\partial^4 w(x,t)}{\partial x^4}+c\frac{\partial w(x,t)}{\partial t}+m\frac{\partial^2 w(x,t)}{\partial t^2}=F(t)\delta\left(x-L_f\right), \tag{6.1}$$

where $w(x, t)$ is displacement of the beam in transverse direction, EI is flexural rigidity, m is mass per unit length of the beam and c is viscous damping coefficient. Using expansion theorem, the displacement of the beam can be written as follows

$$w(x,t)=\sum_{j=1}^{\infty}a_j(t)\phi_j(x), \tag{6.2}$$

where $\phi_j(x)$ is the j^{th} trial function. Utilizing a single trial function and substituting this into Eq. 6.1 results in the following ordinary differential equation

$$EIa(t)\frac{d^4\phi(x)}{dx^4}+c\dot{a}(t)\phi(x)+m\ddot{a}(t)\phi(x)=F(t)\delta\left(x-L_f\right). \tag{6.3}$$

Multiplying Eq. 6.3 by $\phi(x)$ and integrating over the spatial domain the following equation is obtained

$$m_{eq}\ddot{a}(t)+c_{eq}\dot{a}(t)+k_{eq}a(t)=F(t)\phi\left(L_f\right), \tag{6.4}$$

where

$$m_{eq}=\int_0^L m\phi(x)^2dx, \tag{6.5}$$

$$c_{eq}=\int_0^L c\phi(x)^2dx, \tag{6.6}$$

$$k_{eq}=\int_0^L EI\phi(x)\frac{d^4\phi(x)}{dx^4}dx. \tag{6.7}$$

Figure 6.1 shows the deformed shape of the crack beam at two different time instants. Due to breathing effect of the edge crack, the beam behaves as if it is an undamaged beam for some period of a cycle; whereas, in the rest of the cycle it behaves as a beam with an open edge crack. Consequently, beam with a breathing edge crack can be represented as a SDOF system with a piecewise linear stiffness element (or gap element) as shown in Fig. 6.2.

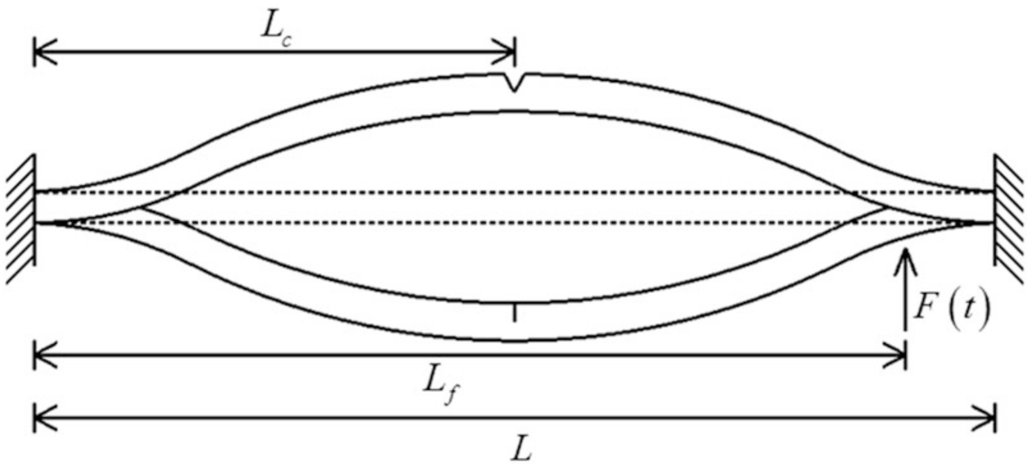

Fig. 6.1 Beam with a breathing edge crack

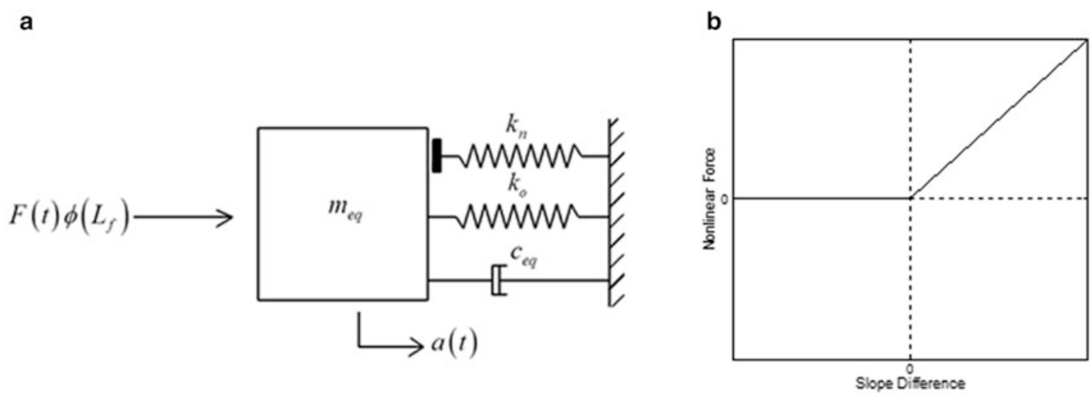

Fig. 6.2 (**a**) SDOF representation of a beam with a breathing edge crack, (**b**) Nonlinear force due to piecewise linear stiffness

Since the crack beam can be represented by two linear systems, two different trial functions corresponding to these two states are required. For the period of vibration where the crack is closed, the first eigenfunction of the undamaged beam is used as a trial function; whereas, the first eigenfunction of a beam with an open crack is used in the case of open crack. The details and derivation of these eigenfunctions can be found in [13], where the response of the left and right sides of the beam with respect to the crack are treated separately. Therefore, the first eigenfunction of a beam with an open crack is composed of two functions named as $\psi_L(x)$ for the beam segment on the left side of the crack and $\psi_R(x)$ for the beam segment on the right side of the crack. Utilizing the first eigenfunction of a beam with an open edge crack and applying Galerkin's Method, k_o and k_n can be obtained as follows,

$$k_o = EI\left(\int_0^{L_c} \psi_L(x)\frac{d^4\psi_L(x)}{dx^4}dx + \int_{L_c}^{L} \psi_R(x)\frac{d^4\psi_R(x)}{dx^4}dx\right), \tag{6.8}$$

$$k_n = k_{eq} - k_o. \tag{6.9}$$

Equation of motion of the nonlinear system given in Fig. 6.2 can be given as follows

$$m_{eq}\ddot{a}(t) + c_{eq}\dot{a}(t) + k_o a(t) + f_n(t) = F(t)\phi\left(L_f\right), \tag{6.10}$$

where $f_n(t)$ is the nonlinear force which depends on the slope difference. In this study, slope difference at the crack location of a beam with an open edge crack is used in order to identify the contact and separation of the piecewise linear stiffness.

Positive slope difference implies a closed crack; thus, a nonzero nonlinear force; whereas, a negative slope difference implies an open crack; hence, zero nonlinear force. Therefore, $f_n(t)$ can be written as

$$f_n(t) = \begin{cases} k_n a(t) \ \ if \quad a(t)\left(\frac{d\psi_R}{dx} - \frac{d\psi_L}{dx}\right)\Big|_{x=L_c} > 0 \\ 0 \qquad if \quad a(t)\left(\frac{d\psi_R}{dx} - \frac{d\psi_L}{dx}\right)\Big|_{x=L_c} < 0 \end{cases}. \tag{6.11}$$

6.3 Application of Harmonic Balance Method

Letting $\theta = \omega t$, $a(t)$ can be written as follows utilizing multi harmonics

$$a(\theta) = a_0 + \sum_p a_{cp} cos(p\theta) + \sum_p a_{sp} sin(p\theta), \tag{6.12}$$

where a_0, a_{cp} and a_{sp} are the bias term, coefficient of sine and cosine components, respectively. Similarly, nonlinear forcing f_n can be written as

$$f_n(\theta) = f_{n0} + \sum_p f_{ncp} cos(p\theta) + \sum_p f_{nsp} sin(p\theta), \tag{6.13}$$

where

$$f_{n0} = \frac{1}{2\pi}\int_0^{2\pi} f_n(\theta)\, d\theta, \tag{6.14}$$

$$f_{ncp} = \sum_p \left(\frac{1}{\pi}\int_0^{2\pi} f_n(\theta) cos(p\theta)\, d\theta\right), \tag{6.15}$$

$$f_{nsp} = \sum_p \left(\frac{1}{\pi}\int_0^{2\pi} f_n(\theta) sin(p\theta)\, d\theta\right). \tag{6.16}$$

Substituting Eqs. 6.12 and 6.13 into Eq. 6.10 and collecting sine and cosine terms lead to the following relation for the p^{th} harmonic

$$\begin{aligned} &\left[\left(k_{eq} - m_{eq}\omega^2 p^2\right) a_{sp} - c_{eq}\omega p a_{cp} + f_{nsp} - F_{sp}\right] sin(p\theta) \\ &+ \left[\left(k_{eq} - m_{eq}\omega^2 p^2\right) a_{cp} + c_{eq}\omega p a_{sp} + f_{ncp} - F_{cp}\right] cos(p\theta) + k_{eq} a_0 + f_{n0} = 0, \end{aligned} \tag{6.17}$$

where F_{cp} and F_{sp} are the cosine and sine components of the p^{th} harmonic of the external forcing. From Eq. 6.17, the following set of nonlinear equations are obtained

$$
\begin{gathered}
ka_0 + f_{n0} = 0 \\
-c\omega \begin{bmatrix} 1 & & 0 \\ & \ddots & \\ 0 & & p \end{bmatrix} \begin{Bmatrix} a_{c1} \\ \vdots \\ a_{cp} \end{Bmatrix} + \begin{bmatrix} k - m\omega^2 & & 0 \\ & \ddots & \\ 0 & & k - m\omega^2 p^2 \end{bmatrix} \begin{Bmatrix} a_{s1} \\ \vdots \\ a_{sp} \end{Bmatrix} + \begin{Bmatrix} f_{ns1} \\ \vdots \\ f_{nsp} \end{Bmatrix} - \begin{Bmatrix} F_{s1} \\ \vdots \\ F_{sp} \end{Bmatrix} = 0 \\
\begin{bmatrix} k - m\omega^2 & & 0 \\ & \ddots & \\ 0 & & k - m\omega^2 p^2 \end{bmatrix} \begin{Bmatrix} a_{c1} \\ \vdots \\ a_{cp} \end{Bmatrix} + c\omega \begin{bmatrix} 1 & & 0 \\ & \ddots & \\ 0 & & p \end{bmatrix} \begin{Bmatrix} a_{s1} \\ \vdots \\ a_{sp} \end{Bmatrix} + \begin{Bmatrix} f_{nc1} \\ \vdots \\ f_{ncp} \end{Bmatrix} - \begin{Bmatrix} F_{c1} \\ \vdots \\ F_{cp} \end{Bmatrix} = 0.
\end{gathered}
\tag{6.18}
$$

6.4 Results and Discussion

In order to study the effect of parameters of breathing edge crack, case studies are carried out on a clamped-clamped beam by using five harmonics. For the case studies, the following beam properties are used: $L = 1\,\mathrm{m}$, $I = 2.667 \cdot 10^{-8}\,\mathrm{m}^4$, $E = 206\,\mathrm{GPa}$, $\rho = 7{,}850\,\mathrm{kg/m}^3$, $A = 8 \cdot 10^{-4}\,\mathrm{m}^2$, $\nu = 0.3$, $c_{eq} = 159.24\,\mathrm{Ns/m}$, $L_f = 0.9\,\mathrm{m}$, $F(t) = 100 sin(\omega t)\,\mathrm{N}$.

In Fig. 6.3, fundamental resonance frequencies for different crack ratios and crack locations are plotted. It is observed that as crack ratio increases, the change in fundamental resonance frequency is more significant. Studying Fig. 6.3b, it is observed that for the case of $L_c = 0.2$, which is very close to the location of the sign change in the slope of the beam, the effect of crack ratio on the fundamental resonance frequency is insignificant. Therefore, in crack detection problems, depending on the crack location, fundamental resonance frequency change may not give accurate results; hence, alternative features should be considered for crack detection.

Due to breathing effect of the crack, in some part of a cycle the crack remains open and in the rest of the cycle the crack remains closed. For this reason nonlinear force is almost zero for some period and nonzero in the rest of the cycle as shown in Fig. 6.4, where, the variation of the nonlinear force at the fundamental resonance frequency is plotted for one cycle at crack location of $L_c = 0.2\,\mathrm{m}$. Even though very little change in fundamental resonance frequency is observed for $L_c = 0.2\,\mathrm{m}$ depicted from Fig. 6.3, the nonlinear force is affected significantly as the crack ratio changes.

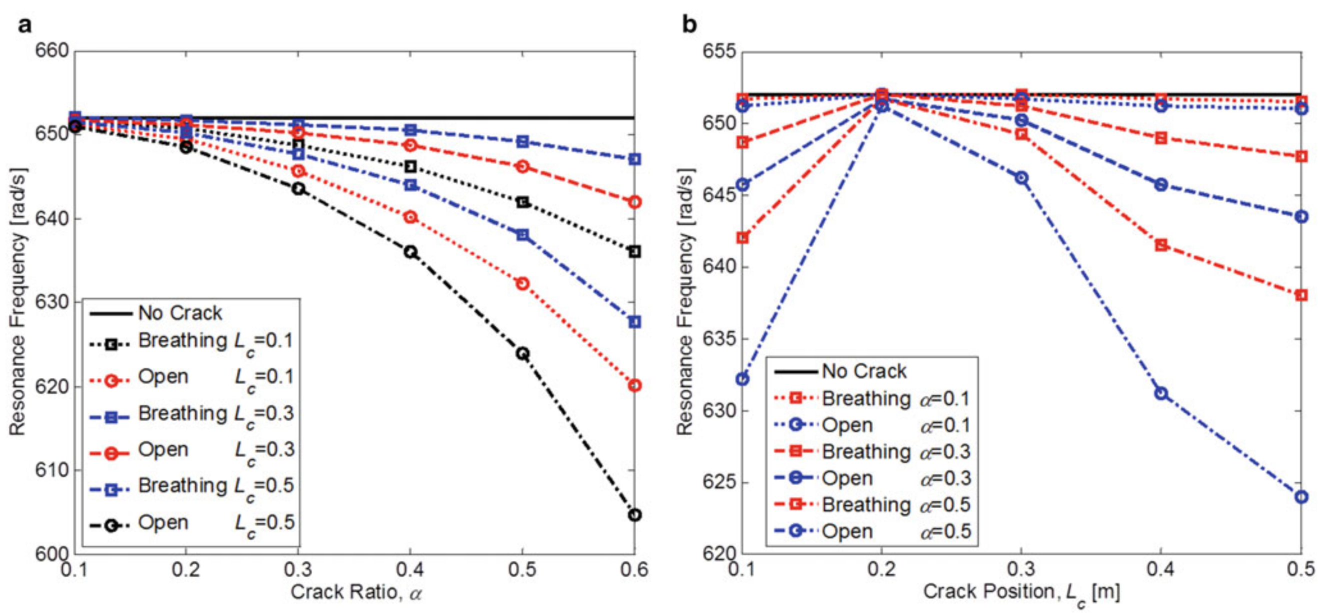

Fig. 6.3 Variation of fundamental resonance frequency with respect to (**a**) crack ratio, (**b**) crack location

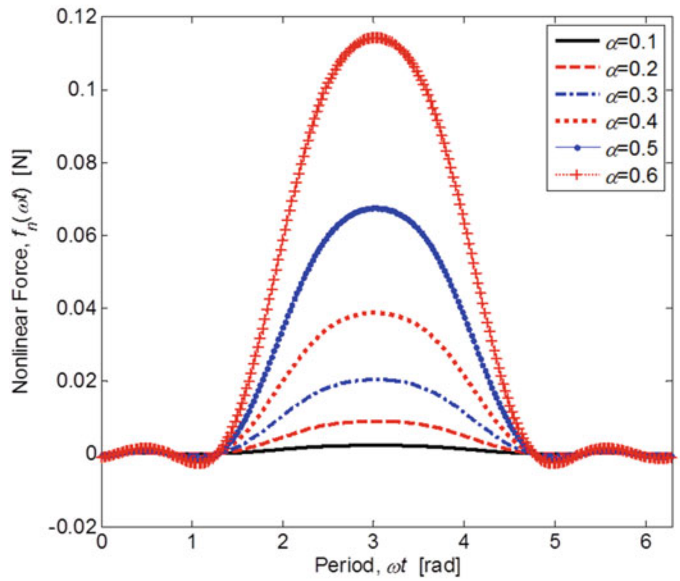

Fig. 6.4 Nonlinear force at fundamental resonance frequency in one cycle, $L_c = 0.2$ m

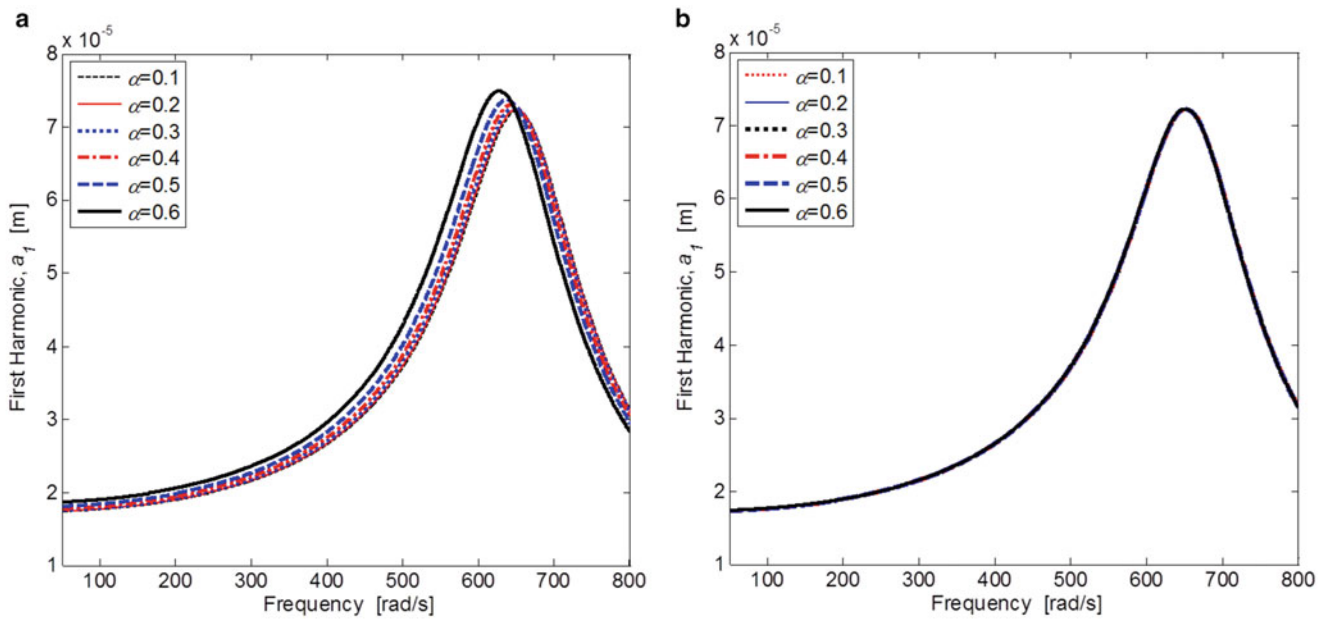

Fig. 6.5 Amplitudes of the 1st harmonic of the modal coefficient versus frequency (**a**) for $L_c = 0.5$ m and (**b**) for $L_c = 0.2$ m

In Fig. 6.5a, b, amplitudes of the first harmonic of the modal coefficient are plotted for different crack ratios for $L_c = 0.5$ m and $L_c = 0.2$ m, respectively. For the case of $L_c = 0.5$ m, the decrease in fundamental resonance frequency can be observed for increasing crack ratios. However, for the case of $L_c = 0.2$ m, no change in the amplitude of the first harmonic of the modal coefficient is observed. However, as shown in Figs. 6.6 and 6.7, bias and higher harmonics of the modal coefficient are affected significantly by the change in crack ratio for the same crack location, i.e. $L_c = 0.2$ m.

Comparison of Figs. 6.5, 6.6 and 6.7 shows that, the most dominant term on the total result is the first harmonic. However, the change in the first harmonic with respect to crack ratio is not as significant as the change in bias term and higher harmonics. To study the effect of crack ratio on the bias term and harmonics of the modal coefficient, the frequency response amplitudes at the fundamental resonance frequency (Figs. 6.5, 6.6 and 6.7 for $L_c = 0.2$ m) are normalized with respect to

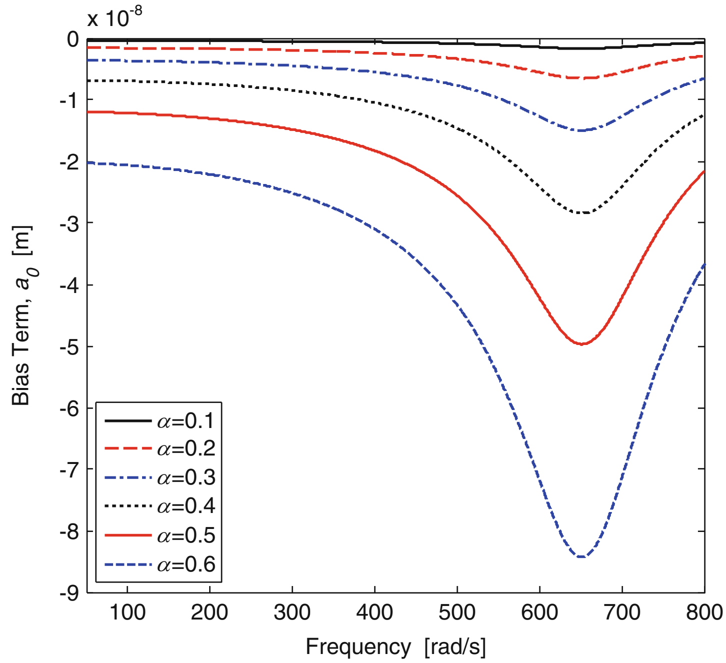

Fig. 6.6 Bias term of the modal coefficient versus frequency, $L_c = 0.2\,\mathrm{m}$

the resonance amplitude obtained for $\alpha = 0.1$. These results are presented in Table 6.1 and Fig. 6.8 for the cases where crack is located at $L_c = 0.1\,\mathrm{m}$, $L_c = 0.2\,\mathrm{m}$ and $L_c = 0.4\,\mathrm{m}$. It is observed from the results that, the effect of crack ratio on bias term, the second and the fourth harmonics is identical to each other; whereas, similar results are obtained for the third and the fifth harmonics. It can be concluded from the results obtained that odd numbered higher harmonics of the modal coefficient are more sensitive to the change in crack ratio; hence, they can be considered as a good feature for crack detection and identification, for this case study. However, it should be noted that, studying Figs. 6.6 and 6.7, the order of magnitude of the bias and second harmonic is approximately three orders greater than the third harmonic, which can be measured with less error compared to the third harmonic. Moreover, as crack location moves towards the center of the beam the multiplication factor increases slightly and for odd harmonics this change is more visible compared to the even harmonics.

Table 6.1 and Fig. 6.8 are prepared according to the amplitudes at fundamental resonance frequency. However, it is observed from Fig. 6.7 that the maximum resonance amplitudes for the higher harmonics occur at frequencies, which are inverse integer multiples of the fundamental resonance frequency. The multiplication factors are also provided at the frequency of maximum amplitude in Table 6.2. Even though the maximum amplitudes occur at different frequencies, the multiplications factors are almost the same. However, as the crack location moves towards the center of the beam the change in amplification ratio is more visible compared to the results obtained at the fundamental resonance frequency (Table 6.1).

6.5 Conclusion

In this study, vibrations of a beam with a breathing edge crack is investigated. Using a single term Galerkin's method, a SDOF piecewise linear system is developed where the nonlinear forcing term depends on the slope difference at the crack location. Case studies show that existence of a crack results in decrease in the fundamental resonance frequency of the beam, which is affected from both the crack ratio and the crack location. It is observed that the fundamental resonance frequency of the beam with a breathing edge crack is higher than the fundamental resonance frequency of the beam with an open edge crack, as expected. However, depending on the crack location the change in the fundamental resonance frequency may become insignificant. Therefore, considering only the change in fundamental resonance frequency does not always give sufficient

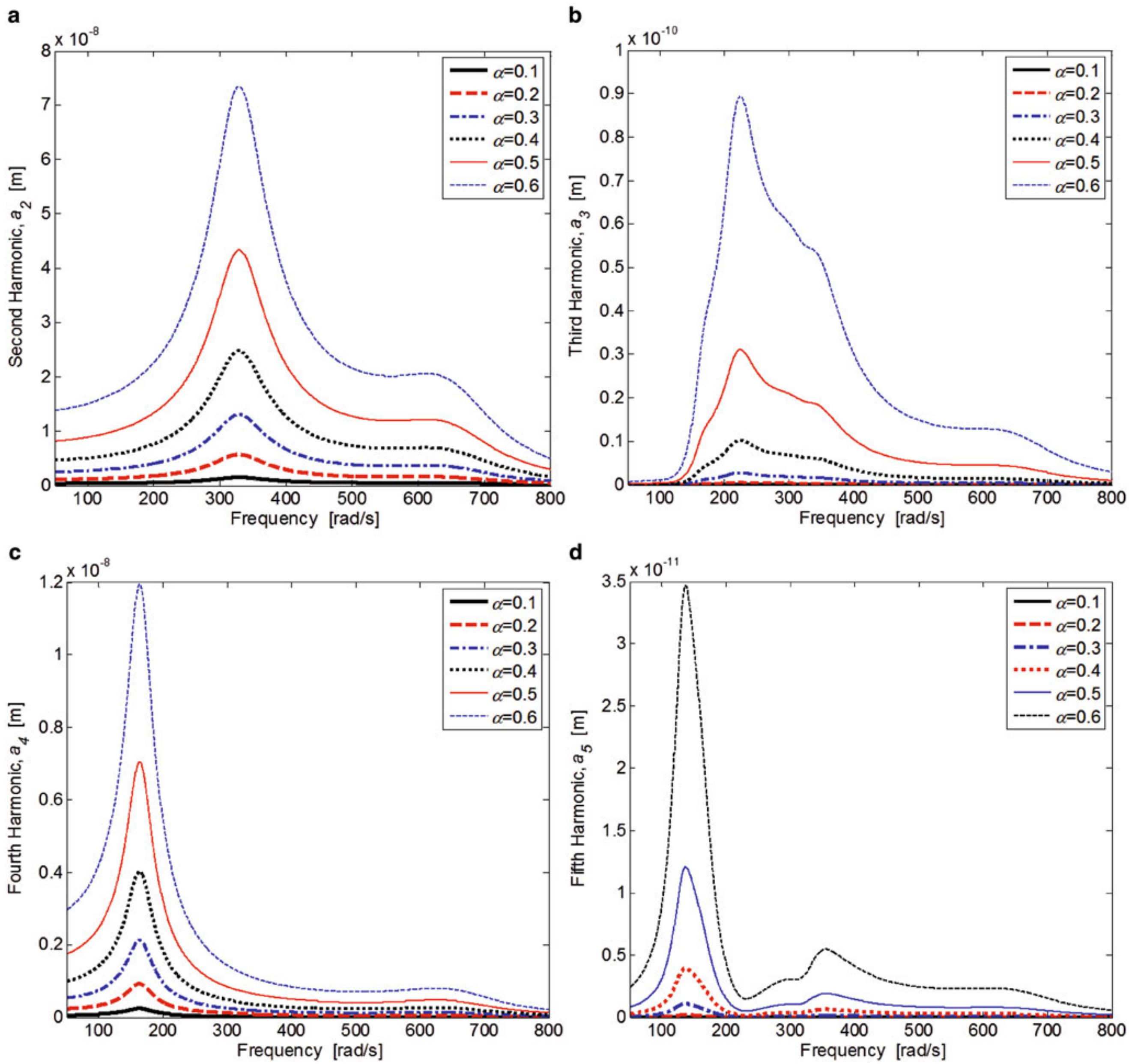

Fig. 6.7 Amplitudes of harmonics of the modal coefficient versus frequency, $L_c = 0.2\,\mathrm{m}$

information for crack detection purposes. Consequently, alternative features are considered for crack detection problems. Effect of crack parameters on nonlinear force f_n is studied and it is observed that change in crack ratio has significant effect on the nonlinear force; however, nonlinear force cannot be measured directly. The harmonics of the modal coefficient are studied and it is observe that the most dominant harmonic on the total response is the first harmonic. However, the effect of crack parameters on the first harmonic is almost insignificant. On the other hand, if bias term and higher harmonics are investigated, it is seen that the effect of crack parameters becomes more significant which can be used as means for crack detection.

Table 6.1 Multiplication factors of bias term and harmonics of the modal coefficient

	$L_c = 0.1\,\mathrm{m}$						$L_c = 0.2\,\mathrm{m}$						$L_c = 0.4\,\mathrm{m}$					
α	0^{th}	1^{st}	2^{nd}	3^{rd}	4^{th}	5^{th}	0^{th}	1^{st}	2^{nd}	3^{rd}	4^{th}	5^{th}	0^{th}	1^{st}	2^{nd}	3^{rd}	4^{th}	5^{th}
0.1	1	1	1	1	1	1	1	1	1	1	1	1	1	1	1	1	1	1
0.2	3.86	1.00	3.84	14.68	3.83	14.69	3.86	1.00	3.86	14.91	3.86	14.89	3.88	1.00	3.87	15.00	3.88	15.00
0.3	8.77	1.00	8.71	75.58	8.71	75.56	8.87	1.00	8.87	78.67	8.87	78.60	8.97	1.00	8.97	80.11	8.97	80.09
0.4	16.35	1.01	16.24	261.45	16.21	261.14	16.86	1.00	16.83	283.50	16.85	283.38	17.22	1.01	17.21	294.07	17.20	293.83
0.5	27.79	1.01	27.62	750.70	27.52	749.43	29.45	1.00	29.42	866.20	29.45	866.47	30.65	1.02	30.66	925.43	30.55	923.78
0.6	45.07	1.02	44.78	1,955.8	44.35	1,948.2	49.96	1.00	49.84	2,487.3	49.95	2,491.4	53.49	1.03	53.50	2,785.2	52.88	2,772.2

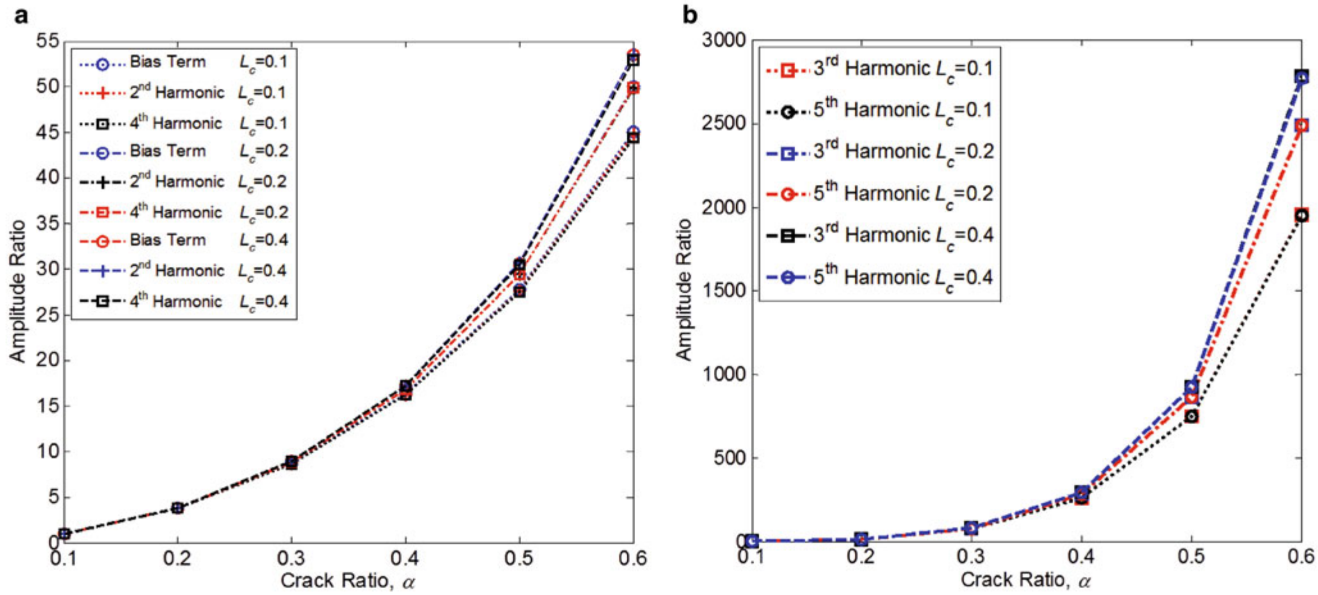

Fig. 6.8 Fundamental resonance amplitude ratios of bias and harmonics of the modal coefficient

Table 6.2 Multiplication factors for higher harmonics at the maximum amplitudes

	$L_c = 0.1\,\text{m}$				$L_c = 0.2\,\text{m}$				$L_c = 0.4\,\text{m}$			
α	2^{nd}	3^{rd}	4^{th}	5^{th}	2^{nd}	3^{rd}	4^{th}	5^{th}	2^{nd}	3^{rd}	4^{th}	5^{th}
0.1	1	1	1	1	1	1	1	1	1	1	1	1
0.2	3.83	14.68	3.83	14.68	3.86	14.90	3.86	14.91	3.88	14.99	3.88	15.00
0.3	8.71	75.41	8.70	75.40	8.87	78.69	8.87	78.69	8.97	80	8.96	79.98
0.4	16.23	260.63	16.22	260.43	16.85	283.68	16.85	283.80	17.21	293.21	17.20	292.93
0.5	27.56	745.85	27.49	744.17	29.46	867.22	29.46	867.53	30.61	918.89	30.53	916.82
0.6	44.68	1933.0	44.33	1, 923.1	49.97	2, 494.0	49.96	2, 494.6	53.37	2, 747.7	52.88	2, 729.9

References

1. Dimarogonas AD (1996) Vibration of cracked structures: a state of the art review. Eng Fracture Mech 55(5):831–857
2. Khiem NT, Lien TV (2001) A simplified method for natural frequency analysis of multiple cracked beam. J Sound Vib 254(4):737–751
3. Aydιn K (2008) Vibratory characteristics of Euler-Bernoulli beams with arbitrary number of cracks subjected to axial load. J Vib Control 14(4):485–510
4. Mermertaş V, Erol H (2001) Effect of mass attachment on the free vibration of cracked beam. In: The 8th international congress on sound and vibration, Hong Kong, China
5. Zhong S, Oyadiji SO (2008) Analytical predictions of natural frequencies of cracked simply supported beam with stationary roving mass. J Sound Vib 311:328–352
6. Mazanoğlu K, Yeşilyurt I, Sabuncu M (2009) Vibration analysis of multiple cracked non-uniform beams. J Sound Vib 320:977–989
7. Chondros TG, Dimarogonas AD, Yao J (1998) A continuous vibration cracked beam vibration theory. J Sound Vib 215(1):17–34
8. Chati M, Rand R, Mukherjee S (1997) Modal analysis of a cracked beam. J Sound Vib 207(2):249–270
9. Chondros TG, Dimarogonas AD, Yao J (2001) Vibration of a beam with a breathing crack. J Sound Vib 239(1):57–67
10. Cheng SM, Wu XJ, Wallace W (1999) Vibrational response of a beam with a breathing crack. J Sound Vib 225(1):201–208
11. Baeza L, Ouyang H (2009) Modal approach for forced vibration of beams with a breathing crack. Key Eng Mater 413–414:39–46
12. Giannini O, Casini P, Vestroni F (2013) Nonlinear harmonic identification of breathing cracks in beams. Comput Struct 129:166–177
13. Batihan AC (2011) Vibration analysis of cracked beams on elastic foundation using Timoshenko beam theory. Master thesis, Middle East Technical University